**Earth and Planetary Science**
https://journals.nasspublishing.com/index.php/eps

ARTICLE

# Columnar Jointing in the Deccan Continental Flood Basalt, India: Implications as a Martian Analogue

***Aditya Das*** [1], ***Subham Sarkar*** [1†], ***Dwijesh Ray*** [1*], ***Rahul Sirvi*** [2]

[1] *Physical Research Laboratory, Planetary Sciences Division, Ahmedabad 380009, India*

[2] *Department of Petroleum Engineering, School of Energy Technology, Pandit Deendayal Energy University, Gandhinagar 382007, Gujarat, India*

[†] *Current address: Department of Earth and Environmental Sciences, Indian Institute of Science Education and Research Berhampur, Odisha 760003, India.*

## ABSTRACT

The continental flood basalt on Earth and the extensive flood basalt provinces on Mars are well recognised for their prominent surface manifestation, which offer valuable insights into the planet's interior activity and evolution. Mars's volcanic provinces are significantly larger than those on Earth; however, the volcanic landforms, particularly the columnar jointing in basalt flows, show some remarkable morphological resemblances. The Deccan trap basalts are characterised by a tholeiite composition with typical iron-rich trend similar to that of Martian basalts. Within the Deccan volcanic province, the columnar jointing includes both colonnade and entablature jointing facies with a more or less consistent hexagonality index (XN:1.34), reflecting its maturity index. A higher cooling rate (0.29 °C/h) contributes to the formation of entablature as compared to colonnade. The morphology of the colonnade is influenced by a uniform cooling mechanism corroborated with the liquid water infiltration during the emplacement of lava. Thus, the columnar jointing in basalt provides insights into the paleoenvironment during lava emplacement. The morphology of columnar basalt on Mars is mainly gained through remote sensing and in situ rover observations. The presence of both colonnade and entablature on Martian columnar basalt also indicates that water was likely prevalent, possibly flooding or ponding during the lava's emplacement. In comparative planetology, incorporating

*CORRESPONDING AUTHOR:
Dwijesh Ray, Physical Research Laboratory, Planetary Sciences Division, Ahmedabad 380009, India; Email: dwijeshray@gmail.com

ARTICLE INFO
Received: 5 January 2025 | Revised: 24 March 2025 | Accepted: 25 March 2025 | Published Online: 1 April 2025
DOI: https://doi.org/10.36956/eps.v4i1.1652

CITATION
Das, A., Sarkar, S., Ray, D., et al., 2025. Columnar Jointing in the Deccan Continental Flood Basalt, India: Implications as a Martian Analogue. Earth and Planetary Science. 4(1): 26–38. DOI: https://doi.org/10.36956/eps.v4i1.1652

new, potential terrestrial analogue materials remains a top priority to validate orbiter data and to strategise for future planetary exploration.

***Keywords:*** Columnar Jointing; Basalt; Deccan; Mars; Terrestrial Analogue

# 1. Introduction

Magmatism and volcanism are the dominant processes responsible for the surface evolution of our inner rocky planets. Since the Noachian and Hesperian epochs, the Martian surface has experienced diverse volcanic activity and is believed to have remained geologically active into the more recent Amazonian epoch [1, 2]. The major volcanic features that exist on Mars include not only shield volcanoes (Olympus Mons), but also channels, flood lavas, calderas, and cones [3]. Additionally, there is evidence of mud volcanoes, hydro or phreatovolcanism, cryovolcanism, and subsurface lavas, which are believed to be prevalent on Mars due to its diverse climatic history and surface/subsurface-hydrosphere-cryosphere interaction [4, 5]. The volcanic resurfacing (manifested mainly by the emplacement of younger lavas) was also common and significantly modified the older, cratered Noachian (>3.5 Ga) terrain on Mars. The discovery of columnar jointing on Mars near the crater walls of Marte Vallis (northeast of Hellas basin) is particularly significant as it provides many invaluable insights into the mode of emplacement of lava, its cooling front, and indirectly implies the past hydrology of Mars [6]. Due to limited exposure and constraints on orbiter image resolution of Mars, terrestrial volcanic analogue sites are crucial for interpreting volcanic landforms and processes of other planets and planetesimals. Additionally, there is a genetic similarity of flood basalt provinces on Earth and Mars (volcanism is linked to a deep mantle, plume-fed), and also resembles the plume-fed continental flood basalt (CFB) on Earth [7].

Though the present conditions of Earth and Mars are markedly different, many geological features appear to be similar during their earliest history (e.g., Mars is thought to have been Earth-like, warm and wet in the past) [8]. In comparative planetology, there is always a continuous effort to comprehend the processes common on Earth and Mars and find a parallel between the two planets. Columnar jointing is common in terrestrial CFBs, and several exposures exist in the Deccan basaltic terrain [9]. The volcanic system of the Deccan traps, characterised by intraplate, plume-driven eruptions, and iron-rich tholeiitic basalts, exhibits several similarities to Martian basalts, despite notable differences. Consequently, in the absence of returned samples from Mars, the Deccan basaltic province may serve as a potential analogue for Martian flood basalts. The field-based data, including mode of occurrences, measurement of width and length of joints, and petrography, are important to decipher the formation process, cooling history, and past climatic conditions during the lava emplacement. Based on a recent field expedition, the columnar jointing in basalts from the Deccan volcanic province in Matanomadh Formation, Kutch, Gujarat, India, offers a unique opportunity to conduct morphometric, petrochemical analyses, allowing for comparisons with Martian counterpart to gain insights into the formation process and the past hydrologic conditions.

# 2. Geological Setting

## Deccan Continental Flood Basalt and Volcanism on Mars

The Deccan CFB erupted during the Cretaceous-Paleogene boundary ($\sim$65 Ma), covering nearly 500,000 $km^2$ in Western and Central India [10]. The popular plume hypothesis largely explains the terrestrial CFB, which discusses magma produced due to the partial melting of deep mantle plumes [11]. Alternate hypotheses also exist and include the sub-continental lithosphere or the decompression melting of a shallow, non-plume mantle [12, 13].

The plume hypothesis argued that the Deccan was emplaced when India passed over a large plume head at the current position of the Reunion hot spot in the Indian Ocean [14]. As there is no large-scale tectonic activity currently known on Mars, Martian volcanism and plume characteristics of Martian basalt are often comparable to the terrestrial hotspots/plumes that resulted in the formation of large igneous provinces and CFB [7].

Besides prominent shield volcanoes on Mars, flood basalts are equally abundant, especially during the early history of Mars (Since Noachian till early Amazonian epoch, ∼4 to 2.5 Ga) [15]. However, based on high-resolution volcanic landform imagery, it is hypothesised that the volcanism peaked during the Hesperian (∼3.7 to 2.9 Ga) [16]. Volcanic eruptions and lava-like flood volcanoes during early Hesperian times are common in the northern lowlands [16]. In contrast, the southern highland is mostly characterised by older-aged Noachian flood basalt. These flood lavas frequently tend to show the cooling joints. The global occurrences of blocks of flood lava plains were confirmed through the orbiter remote sensing [17]. However, the information based on meteoritic studies is limited (the total number of Martian meteorites is small ∼280 nos) and incomplete due to their unknown source/provenance. The majority of volcanic suites of rocks (Shergottite-Nakhla-Chassigny meteorite clan) yield a relatively younger crystallisation age (<2 Ga, based on radiometric age determination of the meteorites), suggesting geologically recent flood volcanism activities [18].

A comparison of Deccan trap basalt and the Martian flood basalt draws some resemblances and differences. Both the terrestrial Deccan Trap volcanic terrain and the Martian flood basalts are within plates, associated with hotspot-related volcanism and erupted enormous volumes of lava within a brief time interval. The Martian flood basalts are linked to a several magnitude higher effusion rate as compared to their terrestrial counterparts. Additionally, the older flood lavas on Mars are believed to be more ancient than those found on Earth (mostly belong to Phanerozoic). Another key distinction is that the terrestrial columnar basalt is largely exposed due to the erosion, while the columnar basalt of Mars is largely exposed at crater wall as a result of later impact events.

# 3. Analytical Techniques

Since the Deccan CFB and the average Martian basaltic crust share spectroscopic and geochemical similarities and have a common genetic linkage, it seems plausible that the geological landform in the volcanic terrain may share some resemblances. Using this example, various analytical approaches were applied to terrestrial Deccan columnar basalt using this analogy to comprehend the mechanism of emplacement, cooling history, and paleoclimatic implications. The analysis of petrography, mineralogy, and whole-rock composition is essential for comprehending rocks, their origins, and possible applications. This process includes thorough descriptions of the rocks, their mineral constituents, textures and the chemical makeup. The morphometric analyses provide the rate of cooling and the mode of emplacement of lava.

## 3.1. Terrestrial

Petrography is carried out using polished thin sections under a polarising microscope (Nikon LV100NPOL) at the Physical Research Laboratory, India. The powdered basalt samples' X-ray diffraction (XRD) analyses were conducted at the Physical Research Laboratory in Ahmedabad, India, using Bruker D2 Phaser benchtop XRD equipment. With current and power ratings of 10 mA and 30 kV, respectively, this XRD system uses a Cu-K excitation and a Ni filter. An agate mortar and pestle were used to grind (up to 250 μ) and homogenise the materials. The samples were scanned at a speed of 0.02° 2θ/s for a 2θ angle range of 10–70°. The accuracy of XRD analyses was better than 0.03° 2θ (w.r.t corundum). Using the phase identification software DIFFRAC.EVA from Bruker (included with the instrument), the peaks of the XRD results were compared with the ICDD-PDF2 database [19].

The major elemental analysis of the finely powdered (grounded up to 60 μ size fractions using the Retsch Planetary Ball Mill PM100) specimen (2 g) was conducted at the Physical Research Laboratory using the methodology of the Panalytical Axios X-ray Fluorescence (XRF) instrument, following the procedural guidelines outlined by Ray and Shukla [20]. The veracity and consistency of our analytical outcomes were evaluated against internationally recognised rock standards, specifically BHVO-2 (Basalt, USGS), G-2 (Granite, USGS), and IF-G (Iron Formation Group, USGS). The results demonstrated a precision and accuracy level better than ±5%, affirming the reliability of our analytical procedures.

### 3.2. MARTIAN

Morphometric analyses of Mars basaltic column are largely dependent on the available images collected by orbiter missions. Based on the altitude of the orbit, the High-Resolution Imaging Science Experiment (HiRISE) camera onboard the Mars Reconnaissance Orbiter (MRO) spacecraft provides a very high spatial resolution of 25–32 cm/pixel [21]. This instrument can effectively resolve features at the meter scale due to its exceptional signal-to-noise ratio and pixel scale.

In this study, we have used two HiRISE images PSP_006774_2020 (centered at Lat: 21.52° Long: 184.35°) and ESP_013871_1945 (centered at Lat: 14.536° Long: 98.513°) showing columnar basalt exposure at a crater wall in the Marte Vallis region and in the right margin of Isidis Basin respectively. No additional processing was done on the images apart from linear stretching on the close-up of the second image using ENVI (version 4.7) software. One HiRISE Digital Terrain model (DTM) was generated using the MARS Système d'Informatio (MarsSI) web platform using the stereo pair HI_013238_1945_013871_1945. This DTM was analysed using QGIS software's 3D visualisation tool.

## 4. Results

### Columnar Jointing: Field Observations, Petrography, Mineralogy and Geochemistry

The Mesozoic basin of Kutch in Gujarat, India, is known as a classic example of a fault-controlled landform resulting from an ancient east-west rift system (**Figure 1a**) [22]. The effect of the Reunion hotspot under the Indian subcontinent led to the formation of a series of extensional fractures, recognised through satellite imagery as faults or lineaments [23]. These fractures ultimately facilitate conductive cooling even after the emplacement of Deccan lavas. The early-formed, rapidly chilled crust in such flows impedes vapour loss, retains fluidity in the lava, and possibly allows for a relatively slower cooling rate of the core. The pulses of endogenous lava transfer encased below the crust are consolidated into an apparently unified core [24]. The distinct pulses that fed these flows can be identified by multi-tiered columnar (entablature) joints, compositional variations, and, in some places, horizontal bands of vesicles that separate the batches of lava in the core [25].

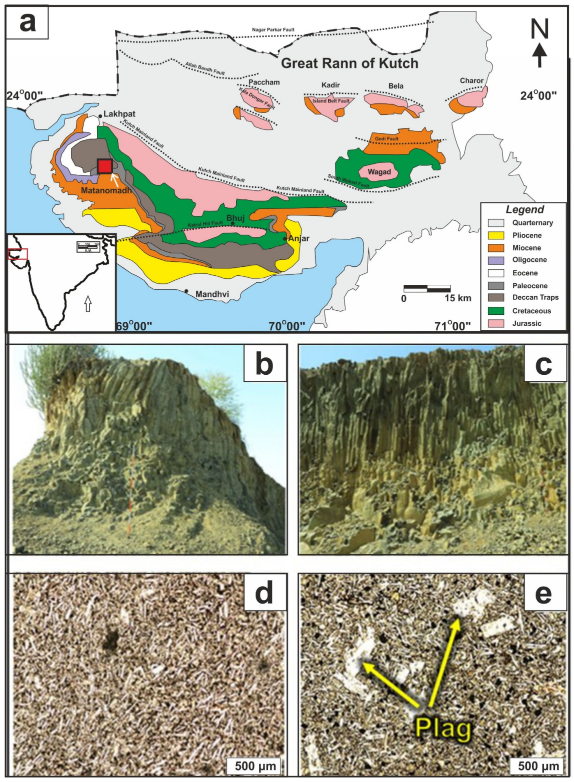


**Figure 1.** (**a**) Location of the study area (marked by red square, base map after Biswas, 1987). Field occurrences of (**b**) entablature and (**c**) colonnade in two different locations. Petrography of basalts (under PPL) from (**d**) entablature and (**e**) colonnade showing the fine-grained texture (a few phenocrysts seen in the latter).

Several types of basaltic columns account for various volcanic landforms, including colonnades and entablature (for a detailed description, see the work of Sheth et al. (2022)) [9]. The columnar basalt in the Matanomadh Formation in Kutch, Gujarat, was exposed in several basaltic quarries and found to be overlain by the tertiary Matanomadh Formation (**Figure 1b**). However, the basement of the columnar basalt is not exposed in the three studied locations (**Figure 1b,c**). No double or multi-tier exposures of entablature and colonnade were found. The lack of conjugate upper entablature and lower colonnade in a single section might suggest a single-unit flow.

The columnar jointing of basalts is studied from three different locations near Matanomadh Formation, India. The two locations were ∼50 m apart, whereas the third location was ∼12 km from the first two. The morphology of columnar jointing resembles colonnade throughout, except in one location where the top layers resemble an entablature-like structure (**Figure 1b**). The basalt colonnades are uniformly thick (average length 6 m and width ∼0.2 m) (**Figure 1c**). The lower contact is not visible and is largely covered by talus. The entablatures show typical curvilinear and are often incised with chevron joints. Although the column's width is nearly consistent, its length is approximately 3 meters, which is shorter than that of other locations.

Petrography of basalt from the colonnade shows the presence of a few scattered plagioclase phenocrysts (**Figure 1f**). Three samples from each field site were selected for petrographic analysis. The texture often resembles a porphyritic type where phenocrysts of plagioclase grains (up to a size of ∼420 µm) are surrounded by smaller and finer grains of plagioclase and pyroxene-dominated groundmass. The petrography of basalt collected from different sectors of the colonnade shows similar mineralogical assemblages (primarily plagioclase+pyroxene and Fe-Ti oxides) with uniform grain sizes (**Figure 1e**). Opaque minerals are mainly titanomagnetite and often ilmenite. Typical skeletal crystals are apparently absent, which is often common in the entablature (**Figure 1e**). The petrography of colonnade and entablature at the boundary appears to be transitional, without any clear demarcation.

The XRD powder diffraction pattern of the basalt sample showed the presence of plagioclase and pyroxene as major minerals (**Figure 2a**) [26–28]. Prominent peaks at 27.96, 28.2, 29.92, 27.75, 30.54, 22.153, 23.82, 30.95, 35.79, 35.90, 42.37, 28.6, 24.63, 35.07, and 35.55° 2θ positions are observed in the powder diffraction pattern. The corresponding d values of these prominent peaks are 3.19, 3.16, 2.98, 3.21, 2.92, 4.01, 3.73, 2.89, 2.51, 2.5, 2.13, 3.61, 2.56, and 2.52 Å. These values were then matched with the published d spacing values of plagioclase 3.20, 3.78, 4.03, 3.66, 2.93 Å [29]. Both enstatite and ferrosilite pyroxene were identified by successfully matching the d spacing values of the minerals at 3.17, 2.50, 2.48Å (enstatite) and 3.21, 2.89, 2.50, 2.58, 2.12, 2.98 Å (ferrosilite) [30, 31]. All the d-spacing values and their corresponding literature values are presented in **Table 1** [29–31].

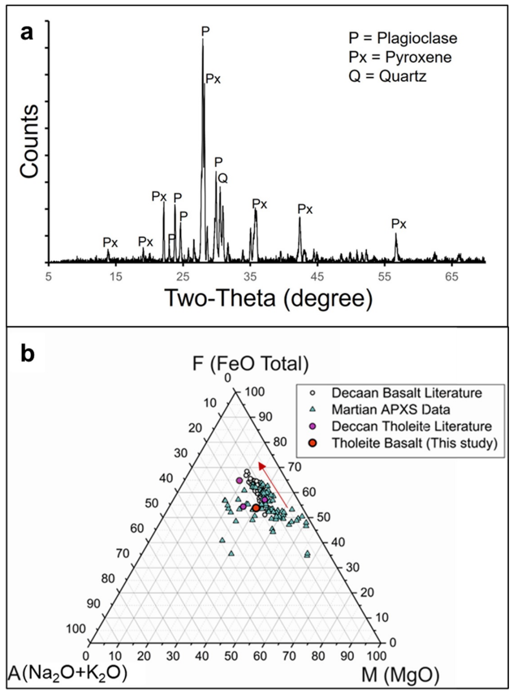


**Figure 2.** (**a**) XRD analyses of the columnar basalt, (**b**) A ($Na_2O$+$K_2O$) F (FeO)M (MgO) diagram to show the compositional plot of the Martian surface (APXS data), Deccan basalt. Additionally, literature Deccan tholeiite from Kutch is also shown for comparison. Arrow shows the Fe-enrichment trend of the Deccan and Martian basalt. Data sources: Ming et al., 2008; Ray et al., 2013; Sen et al., 2009 [26–28].

In the ensuing paragraph, we discussed the whole-rock chemical composition of studied Deccan basalts and compared them with the Martian *in situ* data to find the geochemical analogue. Geochemically, the basalts are tholeiitic with a total alkali-silica content of less than 4 wt%. The $TiO_2$ content ranges from low (0.86–1.55 wt%) to intermediate type (up to 2.8 wt%). The magnesium number (Mg#, calculated as moleMg/mole(Mg+Fe)) ranges from 0.34 to 0.50, suggesting that the magmas are fractionated in nature. In the Alkali-Iron-Magnesium (AFM) diagram, the Deccan basalt from the Matanomadh Formation is compared with the Martian basalt (*in situ* Alpha Particle X-ray Spectrometer (APXS) data from the home plate, Gusev crater) [26]. Both fall under the typical tholeiitic series

**Table 1.** Values for d-spacing (Å) and diffraction angles (°2θ) for identified phases present in the analysed samples with their published data [29–31].

| Interpreted Phase | | °2θ | d (Å) | d (Å) [Literature] |
|---|---|---|---|---|
| Plagioclase | | 27.96 | 3.19 | 3.196$^{a}$ |
| | | 24.63 | 3.61 | 3.663$^{a}$ |
| | | 30.54 | 2.92 | 2.933$^{a}$ |
| | | 22.153 | 4.01 | 4.030$^{a}$ |
| | | 23.82 | 3.73 | 3.780 |
| Pyroxene | Enstatite | 28.2 | 3.16 | 3.175$^{b}$ |
| | | 35.79 | 2.51 | 2.497$^{b}$ |
| | | 35.90 | 2.5 | 2.477$^{b}$ |
| | Ferrosilite | 27.75 | 2.98 | 2.979$^{c}$ |
| | | 29.92 | 3.21 | 3.21$^{c}$ |
| | | 30.95 | 2.89 | 2.892$^{c}$ |
| | | 35.07 | 2.56 | 2.577$^{c}$ |
| | | 42.37 | 2.13 | 2.126$^{c}$ |
| | | 35.55 | 2.52 | 2.504$^{c}$ |

with a distinct Fe-enrichment trend (**Figure 2b**).

The maturation process is the progressive evolution of the polygonal pattern caused by the synchronised adjustment of polygon boundaries as the cracks travel into the cooling body [32]. As the pattern evolves, little columns with fewer than six sides tend to expand at the expense of larger columns (n > 6). The geometry of the column also helps us to understand the maturity of the columns if the columns are not affected by any secondary strains [33]. Indeed, hexagons are the most common in mature patterns. The maturation parameter indicated in

$$X_N = \sqrt{(f_5 + f_7) + 4(f_4 + f_8) + 9(f_3 + f_9) + 16f_{10} + 25f_{11} + \dots} \quad (1)$$

where $X_N$ is known as the hexagonality index of a polygonal pattern and can be used to describe the departure of the distribution from the predicted value of 6 [34]. $f_n$ is the fraction of n-sided polygons in the set.

The maturation process of the polygonal pattern can be quantified by the hexagonality index. For the ultimate stage of maturation $X_N$, should tend toward 0 [32, 34]. The individual column parameter has been estimated using the column width shown in **Figure 3** [35, 36]. The column parameter is given in **Table 2**.

Individual column height and striae are important parameters to explain the formation mechanism consistency of convective cooling and describe columnar basalt morphometry [36]. The striae height (The fractures that produce the sides of the columns progress in distinct, sudden increments, which are indicated by chisel-like impressions known as striae) is proportional to the column width of the colonnade [37]. It falls on the contour of constant striae/length ratio (**Figure 3**). The CFB from other known provinces are also plotted for comparison. In a colonnade, the striae height of the individual column is proportional to the width. However, this relation does not always hold for entablature due to the inconsistency in its column width and lack of measurable striae height. Column length and the top areas of entablature are also smaller than those of the colonnade. Measurement of striae height of Martian columnar jointing is beyond the scope of this study due to the coarser HiRISE image resolution and the images acquired during the previous Mars missions.

The hexagonality of the colonnade in this study is 1.34 (yields comparatively a higher value) and suggests a rapid cooling rate and relatively less mature jointing pattern or heterogeneous distribution of stress during the cooling of lava flows [38]. Based on numerical simulation, it is argued that maturity increases the regularity of the polygon and the number of column faces [39]. Additionally, the size of the column often corresponds to the cooling rate; e.g., a smaller column generally indicates faster cooling, while a larger column accounts for a slower cooling rate [40]. Given several constraints (lava properties, emplacement conditions, cooling mechanism), it is difficult to estimate the cooling rate of magma. However, we adopted a simplified model here to evaluate the cooling rate of basaltic magma.

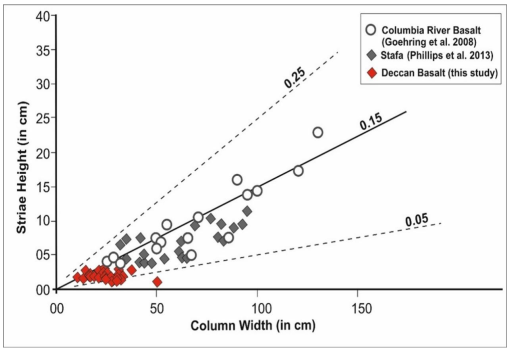


**Figure 3.** The width of the joint shows proportionality with column width. The three contours represent the line of constant striae/length. Other well-recognised columnar basalts from Columbia River basalt and Staffa are included for comparison. Data sources: Goehring et al., 2008; Phillips et al., 2013 [35, 36].

Lore et al. (2001) proposed a model to evaluate the cooling time (t) from a colonnade by

$$t = {L^2}/{\alpha}, \tag{2}$$

where L is the side length of the column, and α is the thermal diffusivity [41].

Using the thermal diffusivity of basalt $10^{-6} m^2 s^{-1}$, the cooling time can be calculated.

Hence, using the cooling time, the cooling rate $\frac{\partial T}{\partial t}$ can be calculated by

$$\frac{\partial T}{\partial t} = \left(1 - \frac{1}{e}\right) \times \frac{T_0}{t}, \tag{3}$$

Where $\frac{\partial T}{\partial t}$ is the cooling rate, e is the natural constant (represents the time for a material to fall to 1/e of the initial temperature) and e is approximately equal to 2.718, $T_0$ is the eruption temperature [41]. For basalts, the temperature is 1200 °C. The cooling rate observed for our columnar lavas ranges from 0.073 °C per hour to 0.29 °C per hour (See **Supplementary Table S1**). The elevated cooling rate aligns well with the entablature.

# 5. Discussion

## 5.1. Formation of Columnar Jointing in Deccan CFB

The formation mechanism of columnar basalt invokes several explanations: (a) contraction of the lava as it cools after the emplacement [42], (b) convection due to diffusion and heat removal from the interior of flow [32], (c) large-scale supercooling due to water flooding [43], and (d) crystallisation-induced melt migration and solidification [44]. Several intrinsic and external factors also play an important role in the formation of columnar lavas. The major controlling internal factors are the magma components, such as temperature, viscosity, effusion flux, and volume. In contrast, the paleotopography and paleoclimate are the major external constraints for basaltic columnar jointing [45]. Based on the field studies in the Deccan CFB area, the role of meteoric water infiltration has been discussed, and the higher water influx induced the formation of entablature, faster downward growth, and thickening of colonnades [9]. The Deccan CFB exhibits characteristics similar to other CFB regions worldwide, such as the Columbia River basalt, and its key volcanic formations play a crucial in understanding past climate conditions. These features suggest a significant interplay between meteoric waters and the cooling lava flows, suggesting a humid climate characterised by substantial rainfall and effective surface drainage [46–48]. We propose that formations such as entablature with irregular, chevron jointing necessitate convective cooling, which is only feasible with substantial interaction with meteoric waters. This interaction would not only promote the solidification of lava at the surface but also aid in the solidification of dykes at deeper levels. The length and width of the column also vary based on the chemical composition. The alkaline basalt generally has slender columns as viscosity probably inhibits the crack formation to induce the mature columnar jointing, while the columns of the tholeiitic basalts are relatively thicker, forming due to the slower cooling rate [40].

The timing of the eruption of the Deccan Trap volcanics in Kutch encompasses 68–61 Ma [49]. The time interval further suggested that the onset of the terminal phase of Deccan volcanism is almost coeval with the spreading regime at the western Indian Ocean. As the plume head gradually deescalated, the extensional regime in the form of a rifted basin became dominant in the region. This process induced the development of extensional stress, which was gradually transmitted in-

**Table 2.** Number of column sides and their respective frequencies among the 74 columns taken for the calculation.

| | Number of Polygon Sides | | | | | | | Total | n̄ | $X_N$ |
|---|---|---|---|---|---|---|---|---|---|---|
| | 3 | 4 | 5 | 6 | 7 | 8 | 9 | | | |
| **Sample size** | 1 | 23 | 17 | 21 | 11 | 1 | - | 74 | 5.28 | 1.34 |

n̄ is the weighted average sides of the columns and $X_N$ is the calculated hexagonality index based on eq. (i). The plan view photograph of the column, which served as the basis for these calculations, is shown in **Supplementary Figure S1**.

land and resulted in fracturing and jointing. The incisive fracturing and jointing ultimately induced a favourable condition for the formation of columnar jointing of the Deccan lava. The stratigraphic deposition observed in the Matanomadh Formation aligns with this model and is characterised by the Deccan traps that erupted within the Mesozoic rift fill basin in this area, as detailed by Mitra et al. in 2017 [50].

The apparent morphological resemblance of the basaltic column of Deccan CFB in concert with the Martian column thus indirectly infers the thermal history of Mars. The uniform columnar jointing in the colonnade suggests uniform conductive cooling. The entablature in a relatively higher stratigraphic position suggests the increased rate of cooling due to water ingress and access to water across the interior. Based on the jointing pattern, we further infer that the entablature is likely to form when multiple joints meet together. This causes a complex distribution of stress and, hence, irregular and curving columns [51]. The intersecting of multiple jointing with often chevron patterns in the Matanomadh Formation further supported distorted isotherm or broadly undulating in nature due to the increased meteoric water influx. Additionally, the hexagonal jointing and the fracture pattern are also attributed to the thermal contraction [35]. This contraction is likely to be enhanced by conductive cooling and water infiltration along the fracture. The higher water penetration along the fractures largely contributes to the entablature formation on the top [52, 53]. However, the finer constraint on columnar basalt formation on Mars is largely inhibited due to the coarser resolution of images.

## 5.2. Deccan Basalt-A Potential Analogue to Mars?

The Deccan trap CFB shows many resemblances with the Martian basalt and is discussed in this section. Mars is known as a basaltic planet, and the Mars Global Surveyor (MGS) Thermal Emission Spectrometer (TES) data of the Martian surface share a similar spectral characteristic (both the spectral shape and contrast) to the Deccan CFB [54]. The Fe-rich chemical composition of Deccan CFB is consistent with the basaltic Martian meteorite shergottite, making it a potential geochemical analogue (Hagerty and Newsom, 2003). Additionally, the role of a mantle plume (Reunion) feeding the CFB eruption on Deccan and the possible long-lived, mantle plume-induced flood basalts on Mars comprehend the Deccan CFB to be a potential terrestrial analogue to the Martian flood basalt [7, 11]. Milazzo et al. have identified columnar jointing features with flow thicknesses up to 30–40 m on the walls of a large ( 16 km diameter), well-preserved, unnamed crater in Marte Vallis [55]. Additionally, they listed several other locations (adjacent to the Isidis Planitia) that (may) have exposed columnar jointing features. There are occurrences of some radiating, fanning structures associated with the colonnade. The heights of the columns vary between as low as 20 m to >30 m (Column heights were calculated using a digital elevation model based on a pair of HiRISE images; **Figure 4a,b**). The slopes of the columns are 60°–66° and the column widths vary up to the order of 2 m. Some outcrops apparently show multiple tiers of columns, which are in places separated by more massive layers. The majority of the columns on Mars were exposed in the uplifted walls of the impact craters. This further suggested that the target of the impact had an earlier history of flood volcanism. Columnar jointing was developed as inherent and genetically unrelated to the impact [55]. The other occurrences of columnar basalt from Mars were also recognised from the wall of the impact crater in the eastern part of the Isidis Basin (**Figure 4c,d**).

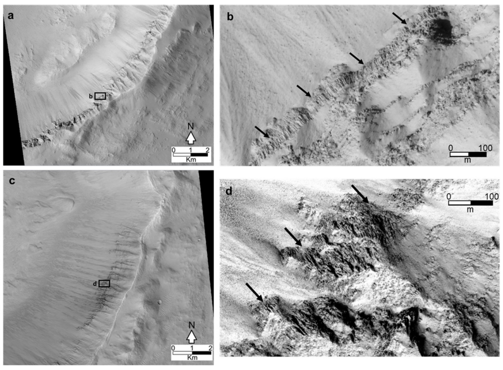


**Figure 4.** (**a**) HiRISE (High Resolution Imaging Science Experiment) image PSP_006774_2020 (Centered at Lat: 21.52° Long: 184. 35°; cropped) showing columnar basalt exposer at crater wall in the Marte Vallis region. (**b**) Close-up of a section of (**a**) showing a well-exposed column (marked by arrows). (**c**) HiRISE image ESP_013871_1945 (Centered at Lat: 14.536° Long: 98.513°; cropped) showing columnar basalt exposure at an impact crater wall located at the right margin of Isidis Basin. (**d**) Close-up of a section of (**c**) showing well-exposed columns (this image is linearly stretched for better visibility).

### 5.3. Columnar Jointing and Past Hydrology

Columnar jointing is one of the enigmatic structures in CFB and can also provide clues to the solidification histories under a particular paleoclimate condition [9]. Based on paleosol and redboles from Decan CFB terrain, the prevailed scenario of emplacement of Deccan flood basalt is favoured for an intermittent intensive and higher tropical rainfall during the Deccan CFB eruption [56, 57]. The higher chemical index of alteration and mafic index of alteration of the intermittent redboles is also consistent with a warm and humid tropical condition [56]. Based on a recent study, the low $\delta 18O_{VSMOW}$ value (mean ∼−12 ± 2‰) of meteoric water compared to the modern mean monsoon rainwater (∼−5‰) in Indian subcontinent further implies a substantially higher rainfall (at least 560–660 mm/year higher) as compared to present day during the Cretaceous-Paleogene boundary in India [57]. The presence of entablature is suggested for a wet spell scenario during the timing of lava emplacement at Deccan CFB. The quench texture in the entablature also further consolidated the view that the meteoric water affected not only the surface but also, to some extent, the subsurface as well [9]. Similar to Earth, the evidence of prolonged fluvial activity is also largely known on early Mars [58]; however, the role of liquid water producing the Martian column is still unconstrained. The existence of drainage channels in several locations, e.g., Elysium Planitia, argues in favour of multiple episodes of aqueous flooding during volcanic activity on Mars [59–61]. Therefore, the role of fluid to induce additional cooling along the fractures and joints of the Martian lavas cannot be fully ignored. Even though the flood basalts on Mars seem to be similar to the CFB on Earth, the duration and the geologic extent of activity are several magnitudes higher, and the volcanic and aqueous flooding cycles are assumed to last for several years on Mars [62].

Although there are interpreted similarities in volcanic styles on Mars, the distinct characteristics of the Martian environment will influence eruption dynamics and the crystallisation of erupted materials [63]. A significant aspect to consider is the impact of Mars' lower atmospheric pressure, averaging 6 mbar at the surface, in contrast to Earth's 1 bar at sea level. Furthermore, the heat loss from the base of lava flows into the underlying surface is governed by the thermal diffusivity of the substrate, which remains consistent across all silicate planets [64]. However, the cooling of the upper surface is affected by atmospheric properties, if present. This reduced atmospheric pressure also causes a 1.5-fold increase in gas velocity and enhances magma fragmentation, resulting in more extensive dispersal of finer volcanic materials during explosive eruptions on Mars compared to Earth [63]. Nevertheless, the Martian lavas are related to higher and longer flow rates with greater preservation potential of volcanic landforms as compared to Earth and the existence of columns indicates the likely sustained presence of liquid water over a span of several decades.

## 6. Conclusions

The columnar jointing in the basalt of Matanomadh Formation, India, shows morphological resemblance (both the entablature and colonnade) to the columnar jointing of Mars. Based on Deccan trap basaltic column, the occurrences of entablature at relatively higher topographic elevation are consistent with substantial meteoric water ingress. With gradual progress downwards, the colonnade started to form. The hexagonality index ($X_N$:1.34) further corroborates the uniform cooling during the lava emplacement. The fine-grained petrographic characters also support rapid chilling of lava due to water ingress. The apparent similarity of morphological jointing pattern of Deccan trap and those found on Mars may suggest a comparable formation mechanism, albeit, the Martian columns are considerably larger in scale. Nonetheless, based on studies of columnar basalts morphology from Earth, the columnar basalts on Mars suggest the water is likely present during the lava emplacement. It appears that water may have been present in a flooded or ponded state during the lava emplacement; however, the source and duration of fluid remain uncertain.

Additionally, the Deccan basaltic provinces in Matanomadh Formation, India, hold significant promise for diverse scientific inquiries in the future of its diverse geology and, to some extent, resemble the early Mars [51, 64–67]. Furthermore, being a probable Martian analogue, this area can serve as an excellent site for testing rovers and other scientific payloads for potential surface exploration and remote sensing techniques.

## Supplementary Materials

The following supporting information can be downloaded at https://journals.nasspublishing.com/public/EPS-1652-Supplementary-Material.docx.

## Author Contributions

Conceptualization, D.R.; methodology, A.D. and S.S.; validation, A.D., S.S., and D.R.; formal analysis, A.D. and S.S.; investigation, A.D., S.S., D.R., and R.S.; resources, R.S.; data curation, A.D. and S.S.; writing—original draft preparation, A.D., S.S., and D.R.; writing—review and editing, D.R; supervision, D.R; project administration, D.R.; funding acquisition, D.R. All authors have read and agreed to the published version of the manuscript.

## Funding

This work was supported by the Department of Space, Government of India.

## Institutional Review Board Statement

Not applicable.

## Informed Consent Statement

Not applicable.

## Data Availability Statement

Most of the analytical data are provided in the main text or in the **Supplementary Material**. Additional data are available from the author upon reasonable request.

## Acknowledgement

We acknowledge the anonymous reviewers whose insightful critiques significantly enhance the quality of the manuscript.

## Conflicts of Interest

We confirm that this manuscript has not been published elsewhere and is not under consideration by another journal. All authors have approved the manuscript and agree with submission to Earth and Planetary Science. We have read and have abided by the statement of ethical standards for manuscripts submitted to Earth and Planetary Science. The authors have no conflicts of interest to declare.

## References

[1] Horvath, D.G., Moitra, P., Hamilton, C.W., et al., 2021. Evidence for geologically recent explosive volcanism in Elysium Planitia, Mars. Icarus. 365, 114499. DOI: https://doi.org/10.1016/j.icarus.2021.114499

[2] Stähler, S.C., Mittelholz, A., Perrin, C., et al., 2022. Tectonics of Cerberus Fossae unveiled by marsquakes. Nature Astronomy. 6(12), 1376–1386. DOI: https://doi.org/10.1038/s41550-022-01803-y

[3] Weitz, C.M., Bishop, J.L., Grant, J.A., 2013. Gypsum, opal, and fluvial channels within a trough of Noctis Labyrinthus, Mars: Implications for aqueous activity during the Late Hesperian to Amazonian.

Planetary and Space Science. 87, 130–145. DOI: https://doi.org/10.1016/j.pss.2013.08.007

[4] Keszthelyi, L.P., Jaeger, W.L., Dundas, C.M., et al., 2010. Hydrovolcanic features on Mars: Preliminary observations from the first Mars year of HiRISE imaging. Icarus. 205(1), 211–229. DOI: https://doi.org/10.1016/j.icarus.2009.08.020

[5] Brož, P., Krýza, O., Wilson, L., et al., 2020. Experimental evidence for lava-like mud flows under Martian surface conditions. Nature Geoscience. 13(6), 403–407. DOI: https://doi.org/10.1038/s41561-020-0577-2

[6] Bhattacharyya, T., Pal, D.K., Lal, S., et al., 2006. Formation and persistence of Mollisols on zeolitic Deccan basalt of humid tropical India. Geoderma. 136(3–4), 609–620. DOI: https://doi.org/10.1016/j.geoderma.2006.04.021

[7] Broquet, A., Andrews-Hanna, J.C., 2023. Plume-induced flood basalts on Hesperian Mars: An investigation of Hesperia Planum. Icarus. 391, 115338. DOI: https://doi.org/10.1016/j.icarus.2022.115338

[8] Wordsworth, R.D., Kerber, L., Plerrehumbert, R.T., et al., 2015. Comparison of ”warm and wet” and ”cold and icy” scenarios for early Mars in a 3-D climate model. Journal of Geophysical Research: Planets. 120, 1201–1219. DOI: https://doi.org/10.1002/2015JE004787

[9] Sheth, H., Duraiswami, R.A., Ghule, V., et al., 2022. Flood basalt structures and textures as guides to cooling histories and palaeoclimates: the Deccan Traps of Saurashtra, western India. Geological Magazine. 159(8), 1415–1436. DOI: https://doi.org/10.1017/S0016756822000279

[10] Self, S., Mittal, T., Dole, G., et al., 2022. Toward understanding Deccan volcanism. Annual Review of Earth and Planetary Sciences. 50, 477–506. DOI: https://doi.org/10.1146/annurev-earth-012721-051416

[11] Duncan, R.A., Richards, M.A., 1991. Hotspots, mantle plumes, flood basalts, and true polar wander. Reviews of Geophysics. 29(1), 31–50. DOI: https://doi.org/10.1029/90RG02372

[12] Hawkesworth, C.J., Gallagher, K., Kirstein, L., et al., 2000. Tectonic controls on magmatism associated with continental break-up: an example from the Paraná–Etendeka Province. Earth and Planetary Science Letters. 179(2), 335–349. DOI: https://doi.org/10.1016/S0012-821X(00)00114-X

[13] Sheth, H.C., 2005. From Deccan to Réunion: no trace of a mantle plume. Special Papers-Geological Society of America. 388, 477.

[14] Mahoney, J.J., Duncan, R.A., Khan, W., et al., 2002. Cretaceous volcanic rocks of the South Tethyan suture zone, Pakistan: implications for the Réunion hotspot and Deccan Traps. Earth and Planetary Science Letters. 203(1), 295–310. DOI: https://doi.org/10.1016/S0012-821X(02)00840-3

[15] Greeley, R., Schneid, B.D., 1991. Magma generation on Mars: Amounts, rates, and comparisons with Earth, Moon, and Venus. Science. 254(5034), 996–998. DOI: https://doi.org/10.1126/science.254.5034.996

[16] Head J.W., III, Kreslavsky, M.A., Pratt, S., 2002. Northern lowlands of Mars: Evidence for widespread volcanic flooding and tectonic deformation in the Hesperian Period. Journal of Geophysical Research: Planets. 107(E1), 3-1–3-29. DOI: https://doi.org/10.1029/2000JE001445

[17] Beyer, R.A., McEwen, A.S., 2005. Layering stratigraphy of eastern Coprates and northern Capri Chasmata, Mars. Icarus. 179(1), 1–23. DOI: https://doi.org/10.1016/j.icarus.2005.06.014

[18] Nyquist, L.E., Bogard, D.D., Shih, C.Y., et al., 2001. Ages and geologic histories of Martian meteorites. In: Kallenbach, R., Geiss, J., Hartmann, W.K. (eds.). Chronology and Evolution of Mars. Space Sciences Series of ISSI, vol 12. Springer: Dordrecht, The Netherlands. pp. 105–164. DOI: https://doi.org/10.1007/978-94-017-1035-0_5

[19] Gates-Rector, S., Blanton, T., 2019. The powder diffraction file: a quality materials characterization database. Powder Diffraction. 34(4), 352–360. DOI: https://doi.org/10.1017/S0885715619000812

[20] Ray, D., Shukla, A.D., 2018. The Mukundpura meteorite, a new fall of CM chondrite. Planetary and Space Science. 151, 149–154. DOI: https://doi.org/10.1016/j.pss.2017.11.005

[21] McEwen, A.S., Eliason, E.M., Bergstrom, J.W., et al., 2007. Mars reconnaissance orbiter’s high resolution imaging science experiment (HiRISE). Journal of Geophysical Research: Planets, 112(E5). DOI: https://doi.org/10.1029/2005JE002605

[22] Biswas, S.K., 1987. Regional tectonic framework, structure and evolution of the western marginal basins of India. Tectonophysics. 135(4), 307–327. DOI: https://doi.org/10.1016/0040-1951(87)90115-6

[23] Arora, K., Srinu, Y., Gopinath, D., et al., 2018. Lineaments in Deccan basalts: The basement connection in the Koyna-Warna RTS Region. Bulletin of the Seismological America. DOI: https://doi.org/10.1785/0120180011

[24] Lamur, A., Lavallée, Y., Iddon, F.E., et al., 2018. Disclosing the temperature of columnar jointing in lavas. Nature Communications. 9(1), 1432. DOI: https://doi.org/10.1038/s41467-018-03842-4

[25] Kale, V.S., Chatterjee, P., Pande, K., 2020. Emplacement history and evolution of the Deccan

Volcanic Province, India. Episodes Journal of International Geoscience. 43(1), 278–299. DOI: https://doi.org/10.18814/epiiugs/2020/020016

[26] Ming, D.W., Gellert, R., Morris, R.V., et al., 2008. Geochemical properties of rocks and soils in Gusev Crater, Mars: Results of the Alpha Particle X-ray spectrometer from Cumberland Ridge to Home Plate. Journal of Geophysical Research. 113, E12S39. DOI: https://doi.org/10.1029/2008JE003195

[27] Ray, D., Misra, S., Widdowson, M., et al., 2013. A common parentage for Deccan Continental Flood basalt and Central Indian Ocean Ridge Basalt? A geochemical and isotopic approach. Journal of Asian Earth Sciences. 84(4). DOI: https://doi.org/10.1016/j.jseaes.2013.12.015

[28] Sen, G., Bizimis, M., Das, R., et al., 2009. Deccan plume, lithosphere rifting, and volcanism in Kutch, India. Earth and Planetary Science Letters. 277(1–2), 101–111. DOI: https://doi.org/10.1016/j.epsl.2008.10.002

[29] Armbruster, T., Bürgi, H.B., Kunz, M., et al., 1990. Variation of displacement parameters in structure refinements of low albite. American Mineralogist. 75(1–2), 135–140.

[30] Pollack, S.S., Ruble, W.D., 1964. X-ray identification of ordered and disordered ortho-enstatite. American Mineralogist. 49(7–8), 983–992.

[31] Turnock, A.C., Lindsley, D.H., Grover, J.E., 1973. Synthesis and unit cell parameters of Ca-Mg-Fe pyroxenes. American Mineralogist. 58(1–2), 50–59.

[32] Budkewitsch, P., Robin, P.Y., 1994. Modelling the evolution of columnar joints. Journal of Volcanology and Geothermal Research. 59(3), 219–239. DOI: https://doi.org/10.1016/0377-0273(94)90092-2

[33] Mondal, T.K., Chowdhury, A., Sain, A., et al., 2022. Understanding the maturity of columnar joints and its spatial relationship with eruptive centre: A critical appraisal from the Rajmahal basalt, India. Physics of the Earth and Planetary Interiors. 326, 106867. DOI: https://doi.org/10.1016/j.pepi.2022.106867

[34] Tanemura, M., Hasegawa, M., 1980. Geometrical models of territory I. Models for synchronous and asynchronous settlement of territories. Journal of Theoretical Biology. 82(3), 477–496. DOI: https://doi.org/10.1016/0022-5193(80)90251-9

[35] Goehring, L., Sletten, R.S., Hallet, B., 2008. Dynamics of polygonal terrain in the Dry Valleys, Antarctica. Proceedings of the 2008 American Geophysical Union Fall Meeting. 15–19 December 2008, San Francisco, USA. p. C22A-08.

[36] Phillips, J.C., Humphreys, M.C., Daniels, K.A., et al., 2013. The formation of columnar joints produced by cooling in basalt at Staffa, Scotland. Bulletin of Volcanology. 75, 1–17. DOI: https://doi.org/10.1007/s00445-013-0715-4

[37] Ryan, M.P., Sammis, C.G., 1981. The glass transition in basalt. Journal of Geophysical Research. 86, 9519–9535.

[38] Goehring, L., Morris, S.W., 2008. Scaling of columnar joints in basalt. Journal of Geophysical Research: Solid Earth. 113(B10). DOI: https://doi.org/10.1029/2007JB005018

[39] Jagla, E.A., 2004. Maturation of crack patterns. Physical Review E. 69, 056212. DOI: https://doi.org/10.1103/PhysRevE.69.056212

[40] Hetényi, G., Taisne, B., Garel, F., et al., 2012. Scales of columnar jointing in igneous rocks: field measurements and controlling factors. Bulletin of Volcanology, 74, 457–482. DOI: https://doi.org/10.1007/s00445-011-0534-4

[41] Lore, J., Gao, H., Aydin, A., 2000. Viscoelastic thermal stress in cooling basalt flows. Journal of Geophysical Research. 105, 23695–23700. DOI: https://doi.org/10.1029/2000JB900226

[42] Hetényi, G., Taisne, B., Garel, F., et al., 2012. Scales of columnar jointing in igneous rocks: field measurements and controlling factors. Bulletin of Volcanology. 74, 457–482.

[43] Gilman, J.J., 2009. Basalt columns: large scale constitutional supercooling? Journal of Volcanology and Geothermal Research. 184(3–4), 347–350. DOI: https://doi.org/10.1016/j.jvolgeores.2009.04.017

[44] Bosshard, S.A., Mattsson, H.B., Hetényi, G., 2012. Origin of internal flow structures in columnar-jointed basalt from Hrepphólar, Iceland: I. Textural and geochemical characterization. Bulletin of Volcanology. 74, 1645–1666. DOI: https://doi.org/10.1007/s00445-012-0623-z

[45] Jin, C., Li, S., Liu, J., 2018. Anisotropic mechanical behaviors of columnar jointed basalt under compression. Bulletin of Engineering Geology and the Environment. 77, 317–330. DOI: https://doi.org/10.1007/s10064-016-0942-y

[46] Long, P.E., Wood, B.J., 1986. Structures, textures, and cooling histories of Columbia River basalt flows. Geological Society of America Bulletin. 97(9), 1144–1155. DOI: https://doi.org/10.1130/0016-7606(1986)97%3C1144:STACHO%3E2.0.CO;2

[47] Lyle, P., 2000. The eruption environment of multi-tiered columnar basalt lava flows. Journal of the Geological Society. 157(4), 715–722. DOI: https://doi.org/10.1144/jgs.157.4.715

[48] Reidel, S.P., Camp, V.E., Tolan, T.L., et al., 2013. The Columbia River flood basalt province: Stratigraphy, areal extent, volume, and physical volcanology. Available from: https://pubs.geoscienceworld.org/gsa/books

/edited-volume/661/chapter-abstract/3807083/The-Columbia-River-flood-basalt-province (cited 30 March 2025).

[49] Courtillot, V., Gallet, Y., Rocchia, R., et al., 2000. Cosmic markers, 40Ar/39Ar dating and paleomagnetism of the KT sections in the Anjar area of the Deccan large igneous province. Earth and Planetary Science Letters. 182(2), 137–156. DOI: https://doi.org/10.1016/S0012-821X(00)00238-7

[50] Mitra, S., Mitra, K., Gupta, S., et al., 2017. Alteration and submergence of basalts in Kachchh, Gujarat, India: implications for the role of the Deccan Traps in the India–Seychelles break-up. Geological Society, London. Special Publications. 445(1), 47–67. DOI: https://doi.org/10.1144/SP445.9

[51] Spry, A., 1962. The origin of columnar jointing, particularly in basalt flows. Journal of the Geological Society of Australia. 8(2), 191–216. DOI: https://doi.org/10.1080/14400956208527873

[52] Grossenbacher, K.A., McDuffie, S.M., 1995. Conductive cooling of lava: columnar joint diameter and stria width as functions of cooling rate and thermal gradient. Journal of Volcanology and Geothermal Research. 69(1–2), 95–103. DOI: https://doi.org/10.1016/0377-0273(95)00032-1

[53] Forbes, A.E., Blake, S., Tuffen, H., 2014. Entablature: fracture types and mechanisms. Bulletin of Volcanology. 76, 1–13. DOI: https://doi.org/10.1007/s00445-014-0820-z

[54] Christensen, P.R., Bandfield, J.L., Hamilton, V.E., et al., 2001. Mars Global Surveyor Thermal Emission Spectrometer experiment: investigation description and surface science results. Journal of Geophysical Research: Planets. 106(E10), 23823–23871. DOI: https://doi.org/10.1029/2000JE001370

[55] Milazzo, M.P., Keszthelyi, L.P., Jaeger, W.L., et al., 2009. Discovery of columnar jointing on Mars. Geology. 37(2), 171

[56] Ghosh, P., Sayeed, M.R.G., Islam, R., et al., 2006. Inter-basaltic clay (bole bed) horizons from Deccan traps of India: Implications for palaeo-weathering and palaeo-climate during Deccan volcanism. Palaeogeography, Palaeoclimatology, Palaeoecology. 242(1–2), 90–109. DOI: https://doi.org/10.1016/j.palaeo.2006.05.018

[57] Ghoshmaulik, S., Bhattacharya, S.K., Hazra, M., et al., 2023. Triple oxygen isotopes in intertrappean fossil woods: Evidence of higher tropical rainfall during Deccan volcanism. Chemical Geology. 121599. DOI: https://doi.org/10.1016/j.chemgeo.2023.121599

[58] Stucky de Quay, G., Kite, E.S., Mayer, D.P., 2019. Prolonged fluvial activity from channel-fan systems on Mars. Journal of Geophysical Research: Planets. 124(11), 3119–3139. DOI: https://doi.org/10.1029/2019JE006167

[59] Jaeger, W.L., Keszthelyi, L.P., McEwen, A.S., et al., 2007. Athabasca Valles, Mars: A lava-draped channel system. Science. 317(5845), 1709–1711. DOI: https://doi.org/10.1126/science.1143315

[60] Keske, A.L., Hamilton, C.W., McEwen, A.S., et al., 2015. Episodes of fluvial and volcanic activity in Mangala Valles, Mars. Icarus. 245, 333–347. DOI: https://doi.org/10.1016/j.icarus.2014.09.040

[61] Hamilton, C.W., Mouginis-Mark, P.J., Sori, M.M., et al., 2018. Episodes of aqueous flooding and effusive volcanism associated with Hrad Vallis, Mars. Journal of Geophysical Research: Planets. 123(6), 1484–1510. DOI: https://doi.org/10.1029/2018JE005543

[62] Keszthelyi, L., McEwen, A.S., 2007. Comparison of flood lavas on Earth and Mars. In: M. Chapman (ed). The Geology of Mars: Evidence from Earth-Based Analogs. Cambridge University Press: Cambridge, UK. pp. 126–150.

[63] Wilson, L., Head, J.W., 1997. Mars: Review and analyses of volcanic eruption theory and relationships to observed landforms. Reviews of Geophysics. 32, 221–263.

[64] Hulme, G., 1982. A review of lava flow processes related to the formation of lunar sinuous rilles. Geophysical Survey. 5, 245–279.

[65] Bhattacharya, S., Mitra, S., Gupta, et al., 2016. Jarosite occurrence in the Deccan Volcanic Province of Kachchh, western India: Spectroscopic studies on a Martian analog locality. Journal of Geophysical Research: Planets. 121(3), 402–431. DOI: https://doi.org/10.1002/2015JE004949

[66] Ray, D., Shukla, A.D., Bhattacharya, S., et al., 2021. Hematite concretions from the Late Jurassic Jhuran sandstone, Kutch, western India: Implications for sedimentary diagenesis and origin of “blueberries” on Mars. Planetary and Space Science. 197. DOI: https://doi.org/10.1016/j.pss.2021.105163

[67] Ray, D., Das, A., Sarkar, S., et al., 2025. Natrojarosite formed in the Matanomadh Formation, Kutch, India: a Na analog of jarosite on Mars. American Mineralogist. DOI: https://doi.org/10.2138/am-2024-9360